International Journal of Pharmaceutics 695 (2026) 126776

Contents lists available at ScienceDirect

International Journal of Pharmaceutics

journal homepage: www.elsevier.com/locate/ijpharm

Hyaluronan-cholesterol core–shell glycerosomes: innovative nanocarriers for mitigating smoke-induced oxidative stress and inflammation in the lungs

Matteo Aroffu [a], Pietro Matricardi [f], Chiara Di Meo [b], Donatella Valenti [a], Maria Ferraro [c], Elisabetta Pace [c], Amparo Nacher [d], Iris Usach [d], José Esteban Peris [d], Octavio Diez-Sales [d], Visar Malaj [e], Rita Abi Rached [a], Jose Luis Pedraz [g,h,i], Ines Castangia [a,*], Maria Manconi [a], Maria Letizia Manca [a]

[a] Department of Scienze della Vita e dell'Ambiente, Drug Science Division, University of Cagliari, Cagliari, Italy
[b] Department of Drug Chemistry and Technologies, Sapienza University of Rome, Rome 00185, Italy
[c] Istituto per la Ricerca e l'Innovazione Biomedica (IRIB), CNR, Via Ugo La Malfa 153, Palermo 90146, Italy
[d] Department of Pharmacy and Pharmaceutical Technology and Parasitology, Faculty of Pharmacy and Food Sciences, University of Valencia, Av. Vicent Andrés Estellés S/n, Burjassot, Valencia 46100, Spain
[e] Department of Economics, Faculty of Economics, University of Tirana, Place Mother Teresa, Tirana 1031, Albania
[f] Department of Biology, University of Tor Vergata, Rome 00185, Italy
[g] NanoBioCel Group, Laboratory of Pharmaceutics, School of Pharmacy, University of the Basque Country (UPV/EHU), Paseo de la Universidad 7, 01006 Vitoria-Gasteiz, Spain
[h] Biomedical Research Networking Center in Bioengineering, Biomaterials and Nanomedicine (CIBER-BBN), 01006 Vitoria-Gasteiz, Spain
[i] Bioaraba, NanoBioCel Research Group, 01006 Vitoria-Gasteiz, Spain

ARTICLE INFO

Keywords:
Pulmonary drug delivery
Glycerosomes
Core-shell nanocarriers
Oxidative stress and inflammation

ABSTRACT

Lungs are constantly exposed to environmental stressors, such as cigarette smoke, which can lead to oxidative stress and inflammation, contributing to the development of chronic lung diseases. To mitigate these conditions, innovative lipid-based nanocarriers, including conventional and core–shell liposomes and glycerosomes, were developed and compared for lung delivery. Curcumin was selected as a potent antioxidant and encapsulated with high yields (> 70%) in the formulated systems. All the nanocarriers were eco-friendly produced by direct sonication, avoiding the use of organic solvents. The core–shell counterparts incorporated a hyaluronan-cholesterol shell without impacting size or polydispersity index, making them suitable for pulmonary administration. Aerosolization studies highlighted conventional and 25 core–shell glycerosomes as the most promising formulations due to their superior nebulization (delivered fraction >95%, fine particle dose >3800 μg, and MMAD values <4.2 μm, ideal for lung targeting). Biocompatibility assessments on A549 and 16HBE cell lines demonstrated good tolerability (cell viability >80%) at non-cytotoxic curcumin concentrations (<20 μM). Moreover, they effectively countered reactive oxygen species production in A549 cells (cell viability >90% after oxidative stress) and mitigated cigarette smoke extract-induced inflammation in 16HBE cells, outperforming free curcumin (pro-inflammatory IL-6 and IL-8 levels were significantly reduced to even below control levels). These findings suggest the potential of curcumin-loaded conventional and core–shell 25 glycerosomes as inhalable drug delivery systems for the treatment of oxidative stress and inflammation associated with smoke exposure.

1. Introduction

Lungs have a prominent role in humans in the exchange of gases with the environment. Because of their role and extremely large surface area, they are continuously exposed to high levels of oxygen (Fröhlich et al., 2016). From oxygen, reactive species are continuously generated from both endogenous (i.e., mitochondria, peroxisomes, and phagocytic cells) and exogenous (i.e. pollution, cigarette smoke, ultraviolet irradiation,

* Corresponding author.
E-mail address: ines.castangia@unica.it (I. Castangia).

https://doi.org/10.1016/j.ijpharm.2026.126776
Received 29 December 2025; Received in revised form 28 February 2026; Accepted 10 March 2026
Available online 13 March 2026

xenobiotics) sources (Barnes, 2020). Physiologically, lungs are well-equipped to counteract these reactive species by enzymes (i.e. superoxide dismutase and catalase) and antioxidants molecules either synthesized in our body (i.e. glutathione, uric acid, ubiquinone, etc.) or introduced with the diet (i.e. vitamins, flavonoids, etc.) (Janciauskiene, 2020; Rogers and Cismowski, 2018). However, when this delicate balance is compromised, oxidative species lead to oxidative stress, damaging vital cellular structures such as lipids, proteins, and nucleic acids. This damage, in turn, contributes to major pulmonary diseases such as asthma, chronic obstructive pulmonary disease (COPD), cystic fibrosis, acute respiratory distress syndrome (ARDS), respiratory infections, and lung cancer (Zuo and Wijegunawardana, 2021). Among the many factors responsible for oxidative stress in the lungs, cigarette smoke accounts for a significant portion as it contains over 4,000 reactive compounds including free radicals and oxidants (Valavanidis et al., 2009).

To address this critical issue, researchers have explored various therapeutic strategies, including the use of natural dietary antioxidants. Polyphenols are a large group of naturally occurring metabolites characterized by the presence of multiple aromatic rings and hydroxyl groups, which confer them potent antioxidant properties (BORS and MICHEL, 2002). The extensive research carried out over these compounds has revealed their potential to mitigate oxidative stress through their ability to 1) scavenge free radicals, 2) inhibit the production of reactive oxygen species (ROS), and 3) modulate cellular signalling pathways involved in the regulation of oxidative stress and inflammation. However, oral intake of polyphenols often results in poor bioavailability and limited tissue distribution (Teng and Chen, 2019). These limitations are considerable when targeting oxidative stress in distal organs like the lungs, as appropriate levels of antioxidants are needed to restore balance (Patton, 2004).

To overcome these challenges, recent investigations have focused on developing innovative delivery systems for polyphenols such as liposomes and glycerosomes (Enaru et al., 2021). These delivery systems can encapsulate and shield these antioxidants from environmental degradation, enhance their solubility in biological fluids, and optimize their delivery to the target organ in a fully biocompatible manner (Fulgheri et al., 2023a, 2023b). Nonetheless, oral administration of these delivery systems may hinder their efficacy due to gastrointestinal passage and hepatic metabolism. Thus, a more direct approach to delivering these systems to the lungs is strongly advised (Le et al., 2020; Muller et al., 2019).

Lung administration is a promising route to maximize local antioxidant availability and target oxidative stress at its source in the lungs. In addition to bypassing hepatic drug metabolism, lung administration offers the advantages of lower doses, reduced systemic exposure, and a faster onset of action than oral administration. In this regard, various researchers have developed liposomes and glycerosomes, among the diverse nanocarrier options currently available, to deliver antioxidants directly to the lungs via inhalation (Aati et al., 2024; Manca et al., 2015; Rached et al., 2025). The list of polyphenols delivered to the lungs by these nanocarriers includes curcumin, quercetin, resveratrol, epigallocatechin gallate, and gingerol, among many others (Lukhele et al., 2023; Yong et al., 2024). Curcumin was selected as a model polyphenol for delivery because of its well-recognized antioxidant and anti-inflammatory activities, which are highly relevant in smoke-related lung injury, where oxidative stress and inflammatory signalling are key drivers of epithelial damage (Aoshiba and Nagai, 2003). Many authors have linked the rationale for curcumin use in smoking-induced lung diseases to multiple mechanisms, including modulation of the PPARγ-NF-κB signaling pathway, inhibition of COX-2 expression, and upregulation of endogenous antioxidant enzymes like superoxide dismutase, catalase, and glutathione peroxidase (Li et al., 2019; Fanoudi et al., 2024; Kalpana et al. 2007). To harness the beneficial properties of curcumin, two novel delivery systems, hyaluronan-cholesterol core–shell liposomes and glycerosomes, were formulated as inhalable nanocarriers to mitigate cigarette smoke-related damage directly at the target site. For their preparation, a hyaluronan–cholesterol nanogel was used. Differently from conventional vesicular systems, the proposed hyaluronan–cholesterol core–shell design was conceived as a hierarchical architecture in which the lipid vesicle acts as the drug-loaded aerosolizable core, while the hyaluronan–cholesterol nanogel forms a functional shell. In fact, its dual hydrophilic-hydrophobic structure enables the cholesterol moiety to anchor into the vesicle bilayer while the hyaluronan chains protrude outward, generating a hydrophilic external layer. This configuration was intended to extend the performance of conventional liposomes and glycerosomes beyond drug encapsulation, by introducing a surface-engineered biointerface that may enhance colloidal stability and biodistribution, modulate particle–mucus interactions, and promote cellular association and potentially interact via CD44 receptors, which are overexpressed on lung epithelial cells (Hussain et al., 2024; Mandal et al., 2013; Nikjoo et al., 2021; Ruwizhi and Aderibigbe, 2020). Direct hydration of the lipid components followed by probe sonication was employed as the preparation method, avoiding thin-film formation or solvent injection steps. This approach simplifies the production process and aligns with sustainable manufacturing practices by minimizing the use of organic solvents (Aroffu et al., 2024; Aroffu et al., 2025). The physicochemical and antioxidant properties were assessed to establish the performance of these novel carriers for antioxidant delivery. A thorough aerodynamic characterization was performed using the Next Generation Impactor, anticipating a direct administration of the formulations to the lungs. Lastly, *in vitro* studies were conducted on two different pulmonary cell lines to assess the protective effects against oxidative stress and inflammatory responses induced by exposure to cigarette smoke extract.

2. Material and methods

2.1. Materials

Phospholipon 90G (P90G) was kindly provided by AVG srl (Milan, Italy), the Italian provider for Lipoid GmbH (Ludwigshafen, Germany). Hyaluronan-cholesterol was synthesized at the Sapienza University of Rome (Italy), according to section 2.3. Curcumin, glycerol, phosphate buffer solution (PBS, pH 7.4), and all the other analytical-grade materials were purchased from Sigma-Aldrich (Milan, Italy). Reagents and plastics for cell cultures were purchased from Life Technologies Europe, (Monza, Italy).

2.2. Synthesis of hyaluronan-cholesterol derivative

The procedure for the synthesis of the hyaluronan-cholesterol derivative was based on previous studies (García et al., 2025; Montanari et al., 2017, 2013). Briefly, at first the cholesterol bromo-butyric derivative was prepared allowing cholesterol (1.3 mmol) to react with 4-bromo-butyric acid (3.9 mmol), 1–3-dimethylaminopropyl-3-ethyl-carbodiimide hydrochloride (3.9 mmol) and 4-(dimethylamino) pyridine (0.65 mmol) in dichloromethane (10 mL) at room temperature, under stirring, overnight. The product CH-Br was purified by column chromatography. To obtain a hyaluronan-cholesterol derivative at the derivatization degree of 15% (mol/mol), hyaluronan tetrabutylammonium salt (200 mg) and CH-Br (26 mg) were dissolved in N-methyl-2-pyrrolidone (12 mL). The reaction was kept under constant stirring at 38 °C for 48 h. Unreacted reagents were removed by exhaustive dialysis (Visking tubing, molecular weight cut-off: 12–14 kDa) against water, and the hyaluronan-cholesterol derivative was obtained as a dry powder by freeze-drying. The successful derivatization of hyaluronan with cholesterol and the corresponding derivatization degree (15% mol/mol) were determined by ^{1}H NMR spectroscopy, by comparing the integration of characteristic proton signals of the cholesterol moiety with those of the hyaluronan backbone, as previously described (Montanari et al., 2013; Montanari et al., 2017). This substitution level was selected based

on previous systematic investigations on hyaluronan–cholesterol derivatives, in which different degrees of derivatization were evaluated and 15% was found to provide stable nanohydrogel formation and suitable physicochemical properties (Montanari et al., 2013; Montanari et al., 2017).

2.3. Preparation of nanogels

The nanogels were prepared by dispersing hyaluronan-cholesterol polymer (10 mg) in 10 mL of either PBS or glycerol-PBS at different glycerol concentrations (12.5, 25, and 50% v/v), followed by magnetic stirring overnight at room temperature to allow complete nanogel formation. The dispersions were then autoclaved (Vapor Matic 770, Milan, Italy), under a standard sterilizing cycle (121 °C for 20 min). Nanogels prepared in PBS were used for the preparation of core–shell liposomes, whereas nanogels prepared in glycerol–PBS were used for the preparation of core–shell glycerosomes. For simplicity, formulations are referred to throughout the manuscript as 12.5, 25, and 50 glycerosomes, corresponding to glycerosomes prepared using 12.5%, 25%, and 50% v/v glycerol in the hydration medium, respectively. This nomenclature is used consistently in all figures and tables.

2.4. Preparation of conventional or core–shell liposomes and glycerosomes

The nanocarriers, whether they were enriched with nanogels or not, were prepared by direct hydration of the lipid phase followed by probe sonication, as previously described (Aroffu et al., 2024; Aroffu et al., 2025). Briefly, P90G (120 mg/mL) and curcumin (5 mg/mL) were weighed directly in glass vials. The lipid phase was hydrated with PBS or glycerol–PBS at different glycerol concentrations (12.5, 25, and 50% v/v) to obtain conventional liposomes or glycerosomes, respectively. Core-shell liposomes and glycerosomes were prepared instead by hydrating the lipid phase with the nanogel dispersions previously prepared (with PBS or glycerol-PBS) according to section 2.3. After 1-hour hydration, all the systems were sonicated 25 + 25 cycles (05 on, 02 off, 14 μm amplitude) using a Soniprep 150 sonicator (MSE Crowley, London, United Kingdom). All the samples were allowed to cool down for 1 min between the cycles to prevent overheating.

2.5. Characterisation of nanogels, conventional liposomes and glycerosomes, and core–shell liposomes and glycerosomes

2.5.1. Physico-chemical properties

Mean diameter, polydispersity index, and zeta potential were assessed with the Zetasizer Ultra (Malvern Instrument, UK). Dynamic light scattering was used to determine size (mean diameter or hydrodynamic diameter) and size distribution (polydispersity index), whereas phase analysis light scattering and the patented mixed-mode measurement were used to assess the magnitude of the repulsion or attraction between the nanocarriers in dispersions (zeta potential). The analyses were carried out at room temperature in triplicate.

2.5.2. Long-term stability

The physical stability of the formulations was evaluated as a preformulation assessment. Samples were stored at refrigerated conditions (4 °C), which are commonly adopted for lipid-based vesicular systems to minimize phospholipid degradation and aggregation phenomena. The mean diameter, polydispersity index, and zeta potential were monitored monthly using the Zetasizer Ultra (Malvern Instrument, UK). The stability study was conducted over a period of 7 months, in accordance with previously reported studies on similar lipid vesicles(Castangia et al., 2016; Manca et al., 2013).

2.5.3. Loading efficiency

Unloaded curcumin was removed from conventional and core–shell liposomes and glycerosomes by dialysis. 1 mL of each formulation was loaded into dialysis tubing (Spectra/Por® membranes: 12–14kDa MW cut-off, 3 nm pore size; Spectrum Laboratories Inc., DG Breda, The Netherlands) and dialyzed against distilled water (1000 mL) at room temperature for 4 h, replacing the distilled water every hour. Drug loading efficiency was determined by high-performance liquid chromatography (HPLC) and was expressed as the percentage of drug retained within the nanocarrier after dialysis with respect to the amount of drug initially used. To do so, conventional and core–shell vesicles, before and after dialysis, were disrupted after appropriate dilution with methanol (1:1000 v/v), and the content of curcumin was assayed at 421 nm using a chromatograph Alliance 2690 (Waters, Milan, Italy) and an analytical column XBridge C18 (5 μm, 4.6x150 mm, Waters, Milan, Italy). A ternary mobile phase made of water:acetonitrile:acetic acid (95:4.85:0.15, v/v) was eluted at a flow rate of 0.7 mL/min and the amount of curcumin was calculated after linear regression from a calibration curve ($R^2 = 0.999$) obtained from at least 3 standard solutions.

2.5.4. Cryo-TEM

Vesicle formation and morphology were checked and confirmed by cryogenic transmission electron microscopy (cryo-TEM), using a Tecnai G2 20 twin (FEI) microscope, operating at an accelerating voltage of 200 KeV in a bright-field image mode and low-dose image mode. An aliquot of the sample (3 μL) was applied to glow-discharged 300 mesh TEM grid and used for plunge freezing into liquid ethane on a FEI Vitrobot Mark IV (Eindhoven, The Netherlands). The frozen grid was then transferred to a 626 DH Single Tilt Cryo-Holder (Gatan, France), maintained below − 170 °C (liquid nitrogen temperature) and then transferred to the TEM for visualization (Casula et al., 2021).

2.5.5. Aerodynamic characterization of nebulized conventional and core–shell liposomes and glycerosomes

The aerodynamic performance of the droplets generated by nebulization of the nanocarriers was assessed with the Next Generation Impactor (Copley Scientific Ltd., Nottingham, UK), operating at 15 L/min and with no pre-separator, under the requirements of the European Pharmacopoeia (*European Pharmacopeia 9.0 2.9.44. Preparations For Nebulisation – Characterisation*, n.d.). The nanocarrier dispersions (2 mL) were loaded into the nebulizer of a Pari Boy® SX air jet nebulizer (Pari GmbH, Starnberg, Germany), which was further connected to the induction port of the Next Generation Impactor and actuated by the Pari TurboBoy® compressor. At the end of the nebulization, appropriate volumes of methanol were used to collect the samples from each stage, facilitating the release of curcumin from the phospholipid vesicles before HPLC analysis. Triplicate measurements were made, allowing to determine mass median aerodynamic diameter (MMAD), geometric standard deviation (GSD), delivered (or emitted) fraction (DF), fine particle dose (FPD), and fine particle fraction (FPF) (Arauzo et al., 2021). Mass median aerodynamic diameter (MMAD) is the aerodynamic diameter of 50% of the droplets generated by nebulization. The geometric standard deviation (GSD) is a measure of the width of the size distribution of the generated droplets. The delivered fraction (DF) is the percentage of the metered dose that exits the nebulizer and is actually available to the user. Lastly, the fine particle dose (FPD) and fine particle fraction (FPF) are, respectively, the amount and the percentage of the drug dose delivered by droplets having an aerodynamic diameter < 5 μm.

2.6. In vitro studies on human A549 lung epithelial cells

2.6.1. Cell culturing of A549 cells

The A549 cells were cultured as monolayers under standard conditions (37 °C, 95% air and 5% CO_2), using Dulbecco's Modified Eagle Medium supplemented with foetal bovine serum (10% v/v), penicillin (100 U/mL), and streptomycin (100 μg/mL) as a growth medium (Euroclone S.p.A., Milano).

2.6.2. Biocompatibility

The A549 cells were seeded in 96-well plates at a density of 7.5×10^3 cells/well and incubated under standard conditions. After 24 h, curcumin, in solution or encapsulated in the nanocarriers, was diluted with medium and added to the cells at final concentrations of 5, 10, 20, and 40 μM (Liu et al., 2018; Chen et al., 2010; Lin et al., 2009). Medium alone was added to cells as positive control (100% of viability). After 24 h of incubation, the biocompatibility was evaluated by Aqueous One Solution Cell Proliferation Assay (Promega, Madison, WI, USA), a colorimetric method for determining the number of viable cells. 20 μL of CellTiter 96® AQueous One Solution reagent was added for each well. The plates were incubated for 20 min at 37 °C, the quantity of formazan produced by the cells, which is directly proportional to the number of metabolically active cells, was measured at 490 nm, using a microplate reader at 490 nm (Microplate reader SPECTROstar-Nano (BMG-Labtech, Allmendgrün, Ortenberg). All the experiments were repeated at least three times and in triplicate. The results were expressed as the percentage of cell viability in comparison with non-treated control cells (100% viability).

2.6.3. Protective effect against oxidative stress

The A549 cells were seeded in 96-well plates and incubated under standard conditions until confluence was reached. Medium was then replaced with medium-diluted hydrogen peroxide (1:40.000 v/v). Immediately after adding the hydrogen peroxide, curcumin, either in solution or loaded in the nanocarriers, was added to the cells at the non-cytotoxic concentration of 20 μM. After additional 4 h of incubation, cells were washed with PBS, and the MTS test was used to assess cell viability after oxidative stress conditions according to section 2.6.2.

2.7. In vitro studies on human 16HBE bronchial epithelial cells

2.7.1. Cell culturing of 16HBE cells

The 16HBE cells were cultured as monolayers under standard conditions (37 °C, 95% air and 5% CO_2), using Eagle's minimum essential medium (MEM), supplemented with 10% foetal bovine serum (FBS), 1% MEM (non-essential amino acids), 2 mM L-glutamine and 0.5% gentamicin (all from Euroclone), as a growth medium.

2.7.2. Biocompatibility

The 16HBE cells were seeded in 96-well plates at a density of 10×10^3 cells/well and incubated under standard conditions. After 24 h, curcumin, in solution or encapsulated in the nanocarriers, was diluted with medium and added to the cells at final concentrations of 5, 10, 20, and 40 μM. Medium alone was added to cells as positive control (100% of viability). After 24 h of incubation, the biocompatibility was evaluated by Aqueous One Solution Cell Proliferation Assay (Promega, Madison, WI, USA), a colorimetric method for determining the number of viable cells. 20 μL of CellTiter 96® AQueous One Solution reagent was added in each well. The plates were incubated for 20 min at 37 °C and the quantity of formazan produced by the cells, which is directly proportional to the number of metabolically active cells, was measured at 490 nm using a microplate reader (Microplate reader SPECTROstar-Nano (BMG-Labtech,Allmendgrün, Ortenberg). All the experiments were repeated at least three times and in triplicate. The results were expressed as the percentage of cell viability in comparison with non-treated control cells (100% viability).

2.7.3. Preparation of cigarette smoke extract

Research grade cigarettes (3R4F containing 9.4 mg tar and 0.73 mg nicotine per cigarette) from Kentucky Tobacco Research and Development Centre at University of Kentucky (Lexington, KY). Cigarette smoke extract (CSE) was prepared using a peristaltic pump Watson-Marlow 323 E/D (Rotterdam, The Netherlands). Each cigarette was smoked for 5 min and one cigarette was used to generate 10 mL of solution in PBS. These procedures were performed in the fume hood. The obtained CSE solution was filtered through a 0.22 μm pore filter to eliminate bacteria and large particles. The CSE solution was used within 30 min of preparation. This solution was set as 100% CSE and was opportunely diluted to obtain the desired concentration for each experiment. The concentration of CSE was verified spectrophotometrically, measuring the OD at a wavelength of 320 nm, as previously described (Ferraro et al., 2019).

2.7.4. Detection of the pro-inflammatory cytokines IL-6 and IL-8

Cell culture supernatants were collected and analysed for IL-6 or Il-8 levels. The human IL-6 or IL-8 ELISA kit (Duo Set R&D Systems, Minneapolis, MN, USA) was used according to the manufacturer's protocol. Specifically, 100 μL aliquots of the cell supernatants were tested, with each experimental group measured in duplicate. The data are expressed as pg/mL.

2.8. Statistical analysis of data

Results are expressed as the mean ± standard deviation. Statistical analysis was performed using the Excel software package (Microsoft Corp., Redmond, USA). One-way analysis of variance (ANOVA) followed by Tukey–Kramer post-hoc test was used to identify statistically significant differences among groups. The minimum level of significance chosen was $p < 0.05$.

3. Results

3.1. Characterisation of nanogels, conventional, and core–shell liposomes and glycerosomes

The physicochemical parameters of the nanogels, such as mean diameter, polydispersity index, and zeta potential, were evaluated before their utilization in the formulation of the core–shell liposomes and glycerosomes (Table 1). PBS-nanogels displayed the smallest mean diameter (267 nm), the narrowest polydispersity index (0.27), and the least negative zeta potential (−39 mV) among the nanogels. A concentration-dependent increase in size and polydispersity index was observed instead for the glycerol-nanogels. The 50 glycerol-nanogels had the largest size (716 nm) and highest polydispersity index (0.54), with values statistically different from those of 12 and 25 glycerol-nanogels ($p > 0.05$). By contrast, the zeta potential values did not statistically differ among the formulations and were around −44 mV. It is possible that the addition of increasing concentrations of glycerol modified the nanogel network, primarily altering its swelling behaviour, ultimately leading to the observed changes in particle size and polydispersity but not in zeta potential(Kozlowska et al., 2018; Oelschlaeger et al., 2016).

The mean diameter, polydispersity index, and zeta potential of both empty and curcumin-loaded conventional and core–shell liposomes and glycerosomes were also investigated, along with the encapsulation efficiency of the loaded nanocarriers (Table 2).

Conventional liposomes, 12 glycerosomes, and 25 glycerosomes had smaller mean diameters and were less polydisperse than conventional 50 glycerosomes regardless of being empty or curcumin loaded. The

Table 1
Mean diameter (MD), polydispersity index (PI), and zeta potential (ZP) of empty nanogels. Data are expressed as mean ± standard deviation of at least three independent experiments. Statistical analysis was conducted separately for each parameter, comparing all formulations within the same column. Different letters indicate statistically significant differences ($p < 0.05$).

	MD (nm)	PI	ZP (mV)
PBS-nanogel	267 ± 88^{a}	0.27 ± 0.06^{a}	-39 ± 6^{a}
12 glycerol-nanogel	$378 \pm 102^{a,b}$	0.29 ± 0.12^{a}	-44 ± 6^{a}
25 glycerol-nanogel	423 ± 139^{b}	0.32 ± 0.11^{a}	-43 ± 4^{a}
50 glycerol-nanogel	716 ± 86^{c}	0.54 ± 0.12^{b}	-44 ± 2^{a}

Table 2
Mean diameter (MD), polydispersity index (PI), zeta potential (ZP), and entrapment efficiency (EE) of curcumin-loaded conventional and core–shell liposomes and glycerosomes. Data are expressed as mean ± standard deviation of at least three independent experiments. Statistical analysis was conducted separately for each parameter, comparing all formulations within the same column. Different letters indicate statistically significant differences ($p < 0.05$).

			MD (nm)	PI	ZP (mV)	EE (%)
Conventional	**Empty**	**Liposomes**	116 ± 31^{a}	0.31 ± 0.08^{a}	-22 ± 1^{a}	–
		12 glycerosomes	120 ± 3^{a}	0.28 ± 0.08^{a}	-22 ± 3^{a}	–
		25 glycerosomes	134 ± 3^{b}	0.30 ± 0.02^{a}	-24 ± 2^{a}	–
		50 glycerosomes	159 ± 19^{c}	0.40 ± 0.05^{b}	-22 ± 3^{a}	–
	Curcumin-loaded	**Liposomes**	123 ± 19^{a}	0.27 ± 0.05^{a}	-21 ± 3^{a}	76 ± 10^{a}
		12 glycerosomes	136 ± 3^{b}	0.25 ± 0.04^{a}	-24 ± 1^{a}	77 ± 12^{a}
		25 glycerosomes	156 ± 10^{c}	0.27 ± 0.08^{a}	-26 ± 2^{a}	72 ± 7^{a}
		50 glycerosomes	437 ± 43^{d}	0.49 ± 0.06^{c}	-28 ± 5^{a}	59 ± 7^{b}
Core-shell	**Empty**	**Liposomes**	111 ± 6^{a}	0.27 ± 0.03^{a}	-37 ± 1^{b}	–
		12 glycerosomes	122 ± 3^{a}	0.29 ± 0.04^{a}	-42 ± 2^{b}	–
		25 glycerosomes	137 ± 1^{b}	0.28 ± 0.04^{a}	-43 ± 2^{b}	–
		50 glycerosomes	157 ± 14^{c}	0.37 ± 0.02^{b}	-47 ± 4^{b}	–
	Curcumin-loaded	**Liposomes**	139 ± 31^{b}	0.28 ± 0.02^{a}	-42 ± 3^{b}	81 ± 2^{a}
		12 glycerosomes	166 ± 32^{c}	0.26 ± 0.04^{a}	-42 ± 3^{b}	80 ± 10^{a}
		25 glycerosomes	252 ± 23^{e}	0.31 ± 0.06^{a}	-39 ± 1^{b}	83 ± 3^{a}
		50 glycerosomes	508 ± 10^{f}	0.29 ± 0.03^{a}	-44 ± 3^{b}	77 ± 8^{c}

increasing concentration of glycerol affected the mean diameter of the systems in a concentration-dependent manner, probably due to changes in the bilayers induced by this molecule (Manca et al., 2013). However, after adding curcumin, the mean diameters increased for all the systems compared to their empty counterparts. This effect might be due to curcumin, which is poorly water-soluble and primarily locates in the lipid bilayer of the vesicles, potentially inducing alteration in membrane packing and, thus, their dimensions. The increased heterogeneity of the conventional 50 glycerosomes loaded with curcumin could be attributed to their significantly low encapsulation efficiency (<60%, $p < 0.05$ versus other values). This is likely due to the tendency of curcumin to form aggregates in aqueous media, due to its low solubility, which can be detected by dynamic light scattering, revealing multiple populations of varying size (Shailendiran et al., 2011).

Zeta potential changed significantly from values > -30 mV for conventional formulations to values < -35 mV for all the core–shell formulations, whether they were empty or curcumin-loaded, and whether they were prepared with glycerol or not. A more negative zeta potential is beneficial as it is known to enhance the stability of nanocarriers upon storage (DUPLESSIS et al., 1996).

Adding the nanogel shell into the lipid core had no significant effect on the diameters nor the polydispersity indexes, as empty formulations shared the same values ($p > 0.05$ between the values obtained for conventional empty nanocarriers and core–shell empty nanocarriers). Since the nanogels alone were bigger (Table 1), sonication likely allowed the downsizing of the nanogels, ultimately not affecting the size of the empty core–shell nanocarriers.

Similar to the conventional counterparts, curcumin loading increased the diameters, likely due to the effective incorporation of the hydrophobic drug into the lipid bilayers, as suggested by the high encapsulation efficiencies obtained (80%). Significantly different variations in polydispersity index were recorded only for the core–shell 50 glycerosomes with respect to conventional 50 glycerosomes. Specifically, its significantly lower value suggested the obtainment of a more homogeneous system, probably due to a different nanocarrier conformation achieved by incorporating the nanogel core (Gruber et al., 2022). The significantly higher encapsulation efficiency (80%, $p < 0.05$ versus the value obtained for conventional 50 glycerosomes) aligns with the higher degree of homogeneity obtained (0.27, $p < 0.05$ versus the value obtained for conventional 50 glycerosomes) as it is likely that no population of curcumin aggregates can be detected by dynamic light scattering once it is effectively encapsulated.

3.2. Cryo-TEM analysis

Cryo-TEM analysis was performed to investigate the morphology of the 25 glycerosomes formulations (conventional and core–shell), selected as the most representative systems based on their superior physicochemical, aerosolization, and biological performance. As shown in Fig. 1, both conventional and core–shell glycerosomes exhibited predominantly spherical vesicles with well-defined bilayer structures. The observed vesicle dimensions were consistent with the size range obtained by DLS measurements. Conventional glycerosomes displayed a typical unilamellar morphology with homogeneous contrast. In contrast, core–shell glycerosomes exhibited a slightly more pronounced peripheral contrast at the vesicle interface. Although a distinct thick polymeric shell could not be directly resolved, the observed contrast enhancement is consistent with the presence of the hyaluronan–cholesterol derivative at the vesicle surface, supporting the proposed core–shell organization. These morphological findings are in line with the physicochemical results and support the proposed interfacial localization of the hyaluronan–cholesterol derivative in the core–shell formulations.

3.3. Long-term stability of conventional and core–shell liposomes and glycerosomes

The mean diameter, polydispersity index, and zeta potential of both conventional and core–shell curcumin-loaded liposomes and glycerosomes were monitored as part of the stability studies for 7 months (Fig. 2). In general, both conventional and core–shell formulations followed similar trends across all parameters, with significant differences observed only in a few cases. Specifically, core–shell liposomes and 12 glycerosomes showed signs of instability starting from the 7th month and 5th month, respectively, whereas their conventional counterparts remained stable. On the other hand, conventional and core–shell 25 and 50 glycerosomes remained stable up to 7 months, maintaining unvaried values of mean diameter, polydispersity index, and zeta potential with respect to the initial values ($p > 0.05$). It was thus evident a stabilizing effect of glycerol on the nanocarriers, and especially on the core–shell variants, since its absence (liposomes) or a low concentration (12 glycerosomes) led to huge increases in the size and polydispersity index over time.

3.4. Aerodynamic characterization of nebulized conventional and core–shell liposomes and glycerosomes

The aerodynamic properties of the formulations are critical for their

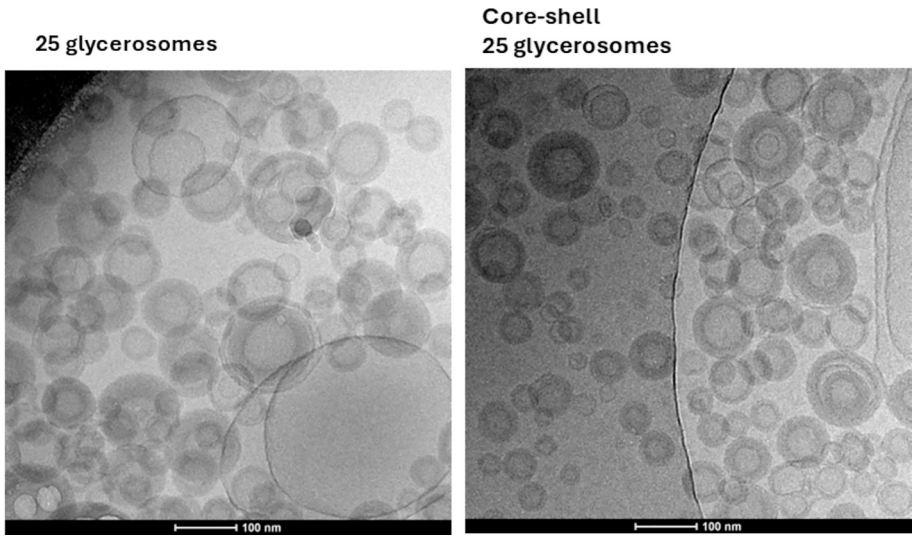

Fig. 1. Representative cryo-TEM images of conventional 25 glycerosomes and core–shell 25 glycerosomes.

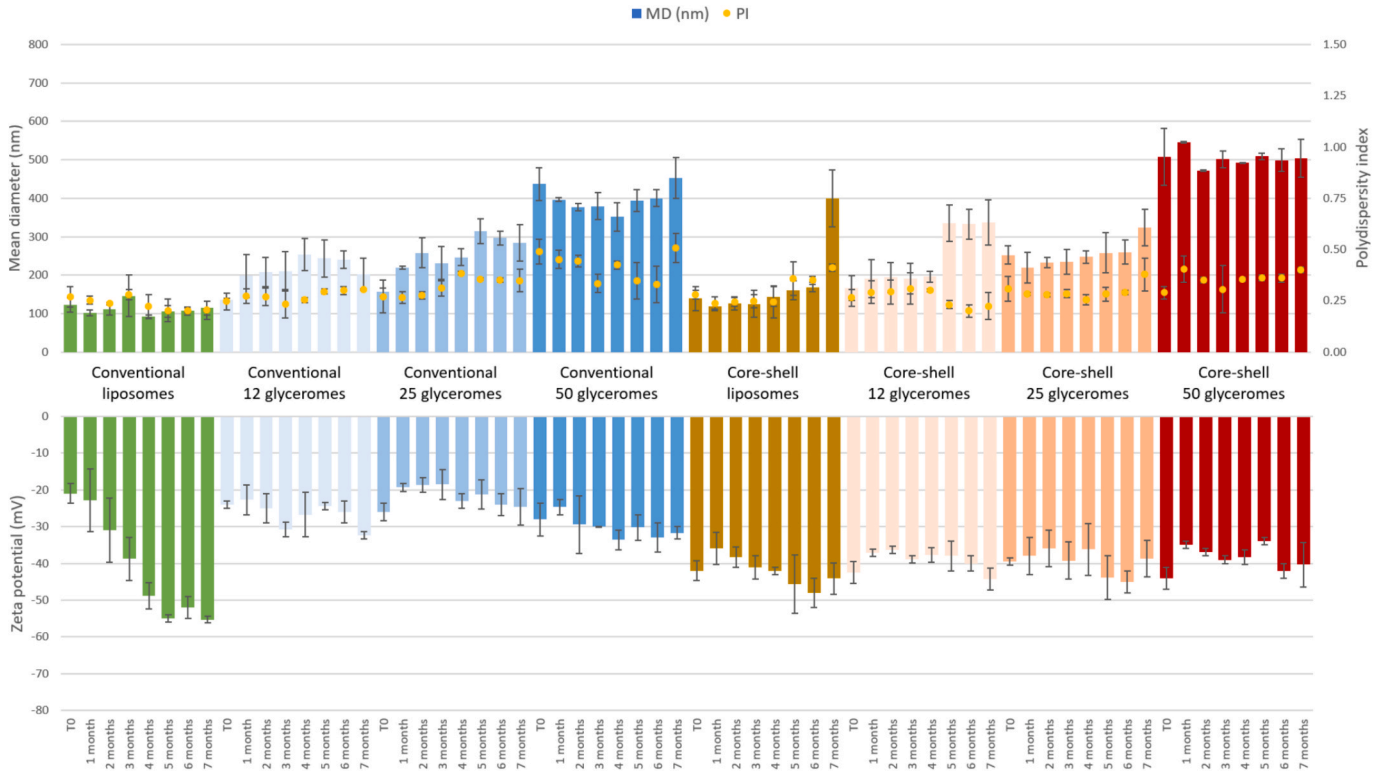

Fig. 2. Mean diameter, polydispersity index, and zeta potential of curcumin-loaded conventional and core–shell liposomes and glycerosomes after preparation, 1, 2, 3, 4, 5, 6 and 7 months. Mean values ± standard deviations, obtained from at least 3 measurements, are reported.

effectiveness in lung delivery. Therefore, conventional and core–shell liposomes and glycerosomes were nebulized using a pneumatic nebulizer and analysed by cascade impaction to determine their Delivered Fraction (DF), Fine Particle Dose (FPD), Fine Particle Fraction (FPF), Mass Median Aerodynamic Diameter (MMAD) and Geometric Standard Deviation (GSD) (Table 3). The DF seemed affected by the viscosity of the formulation in a glycerol concentration-dependent manner, as conventional and core–shell 50 glycerosomes were the only formulations to yield values < 55% ($p < 0.05$ with respect to the values of all the other conventional and core–shell nanocarriers). Thus, an excessively high glycerol concentration (50% w/v and above) may hinder the Pary Boy's nebulization process, negatively influencing total lung deposition. This was reflected by the values of FPD and FPF, which are related to the quantity and the fraction of aerosol particles able to reach the deep lung. Indeed, FPD and FPF were significantly lower for conventional and core–shell 50 glycerosomes with respect to the other formulations. The highest values of FPD and FPF were achieved by conventional and core–shell 25 glycerosomes (> 85% and 3700 μg, respectively), which displayed therefore the best attitude to aerosolization. This might also be related to the smaller MMAD values of these formulations (~4.0 μm), which complied with the MMAD < 5 μm cut-off required to reach deep lung deposition. By contrast, conventional and core–shell 50 glycerosomes had MMAD ~ 4.7–5 μm, which in turn led to FPD ~ 1500 μg and FPF that were barely above 50%. Only the GSD was constant across the

Table 3
Delivered Fraction (DF), Fine Particle Dose (FPD), Fine Particle Fraction (FPF), Median Mass Aerodynamic Diameter (MMAD), and Geometric Standard Deviation (GSD) of curcumin-loaded conventional and core–shell liposomes and glycerosomes. Data are expressed as mean ± standard deviation of at least three independent experiments. Statistical analysis was conducted separately for each parameter, comparing all formulations within the same column. Different letters indicate statistically significant differences ($p < 0.05$).

		DF (%)	FPD (μg)	FPF (%)	MMAD (μm)	GSD
Conventional	**Liposomes**	80 ± 6[a]	2623 ± 12[a]	67 ± 4[a]	4.5 ± 0.2[a]	1.3 ± 0.2[a]
	12 glycerosomes	92 ± 5[a]	3842 ± 36[b]	88 ± 11[b]	4.2 ± 0.1[b]	1.2 ± 0.2[a]
	25 glycerosomes	96 ± 3[a]	3743 ± 51[b]	85 ± 9[b]	4.1 ± 0.1[b]	1.2 ± 0.2[a]
	50 glycerosomes	47 ± 7[b]	1505 ± 22[d]	59 ± 9[a]	4.8 ± 0.2[c]	1.2 ± 0.2[a]
Core-shell	**Liposomes**	83 ± 7[a]	2666 ± 18[a]	72 ± 6[c]	4.3 ± 0.3[a]	1.3 ± 0.1[a]
	12 glycerosomes	86 ± 7[a]	3383 ± 24[c]	84 ± 9[b]	4.0 ± 0.1[b]	1.3 ± 0.2[a]
	25 glycerosomes	96 ± 1[a]	3976 ± 28[b]	88 ± 7[b]	4.1 ± 0.1[b]	1.2 ± 0.2[a]
	50 glycerosomes	55 ± 5[b]	1473 ± 32[d]	51 ± 7[a]	5.0 ± 0.2[c]	1.3 ± 0.3[a]

formulations, either conventional or core–shell, displaying values < 2 that indicate a quite narrow droplet size distribution ideal for lung administration.

3.5. Biocompatibility and oxidative stress protection in A549 cells

The formulations showing the highest aerosolization efficiency were further characterized *in vitro* using A549 cells, a human alveolar epithelial cell line extensively used as a representative model of the pulmonary epithelium in drug delivery research (Foster et al., 1998). Cytotoxic effects were evaluated by exposing cells to curcumin in dispersion or loaded in conventional and core–shell liposomes and glycerosomes at different concentrations (5–40 μM) (Fig. 2, **A**). The highest dose tested (40 μM) was cytotoxic in almost all cases, decreasing the cell viability below 75%. The only exception was represented by core–shell 25 glycerosomes, as they maintained cell viability above 85%. The doses 5–20 μM were well tolerated without significant cytotoxicity (cell viability > 80%) for all the formulations tested. At the lowest dose (5 μM), core–shell 12 and 25 glycerosomes stood as the only formulations able to generate a proliferative effect (cell viability ~ 135%) with statistical differences with the values of all the other formulations tested in the same conditions.

Aiming to compare conventional and core–shell formulations, those showing simultaneously good biocompatibility and aerosol performance were further investigated for their ability to counteract cellular ROS production in A549 cells (Fig. 3, **B**). The use of H_2O_2 significantly reduced cell viability, which with no treatment dropped to ~ 50%. The dispersion of curcumin, used at the non-cytotoxic concentration of 20 μM, partially counteracted ROS production as viability increased up to 66%. However, only the curcumin-loaded nanocarriers, either conventional or core–shell, could restore cell viability to around 100%, confirming their superior and potent antioxidant properties when tested at the same dose. No significant differences were revealed among conventional or core–shell 12 or 25 glycerosomes ($p < 0.05$), probably due to comparable encapsulation efficiencies (>70%).

3.6. Biocompatibility and inflammatory cytokine determination in 16HBE cells

The cytotoxic effect of the most promising formulations was also assessed on healthy bronchial epithelial 16HBE cells at curcumin concentrations in the range 5–40 μM (Fig. 4, **A**).

Among the formulations, conventional liposomes, conventional 25 glycerosomes, and core–shell 25 glycerosomes exhibited cell viability greater than 90%. In contrast, core–shell liposomes, conventional 12 glycerosomes, and core–shell 12 glycerosomes displayed a decrease in cell viability exceeding 15% and were thus excluded from further evaluation for pro-inflammatory cytokine expression.

Given that cigarette smoke is a major cause of oxidative stress, 16HBE cells were exposed to cigarette smoke extract (10% w/v). The ability of the most relevant formulations, based on biocompatibility and aerosolization performance, to counter the oxidant stimulus was evaluated by measuring IL-6 and IL-8 production. Specifically, the conventional and core–shell 25 glycerosomes were tested at a biocompatible curcumin concentration of 5 μM, and their effects were compared to that of the curcumin dispersion (Fig. 4, **B and C**).

All the treatments (curcumin dispersion, conventional 25 glycerosomes, and core–shell 25 glycerosomes) significantly reduced the release of IL-6 and IL-8 induced by cigarette smoke extract. Notably, both conventional and core–shell 25 glycerosomes demonstrated greater efficacy than the curcumin dispersion in mitigating the inflammation induced by the cigarette smoke extract, highlighting the beneficial role of the nanocarrier system in counteracting oxidative stress. Irrespective of the cytokine tested, no significant differences were observed between the two types of nanocarriers, which were equally effective.

4. Discussion

The current research aimed to develop and compare innovative lipid-based nanocarriers, such as conventional and core–shell liposomes and glycerosomes, as promising drug delivery systems for the treatment of lung diseases associated with oxidative stress(Lelli et al., 2017).

To this end, curcumin, a well-known antioxidant compound, was selected as the model drug and encapsulated in nanocarriers with different structural characteristics. Conventional liposomes and glycerosomes were composed of natural ingredients (i.e., phosphatidylcholine, cholesterol, and glycerol), while the core–shell counterparts were achieved by adding a shell of hyaluronic acid and cholesterol. Owing to its previously demonstrated efficacy in topical applications, this nanohydrogel was selected as a promising platform for pulmonary administration (García et al., 2025). The introduction of such a shell did not affect the nanocarrier size and polydispersity indexes, which were narrow and suitable for pulmonary administration (Aroffu et al., 2023). Still, it provided a slightly more negative zeta potential and significantly improved encapsulation efficiency, especially in the case of 25 core–-shell glycerosomes. The presence of hyaluronic acid at the vesicle interface was suggested by the significantly more negative zeta potential observed for core–shell systems compared to conventional vesicles (Aroffu et al., 2023). Zhao and colleagues experienced a similar trend in zeta potential with their hyaluronic acid core–shell nanoparticles (Zhao et al., 2018). However, encapsulation efficiency was unaltered in their study, likely due to the absence of cholesterol in the bilayer and the hydrophilic nature of their cargo. Cryo-TEM analysis further supported the proposed structural organization, revealing spherical vesicles with well-defined bilayers and size distribution consistent with DLS measurements. Core–shell glycerosomes exhibited a slightly enhanced peripheral contrast compared to conventional vesicles, consistent with the localization of the hyaluronan–cholesterol derivative at the vesicle interface. Although the polymeric layer could not be resolved as a distinct thick shell, the combined physicochemical and morphological

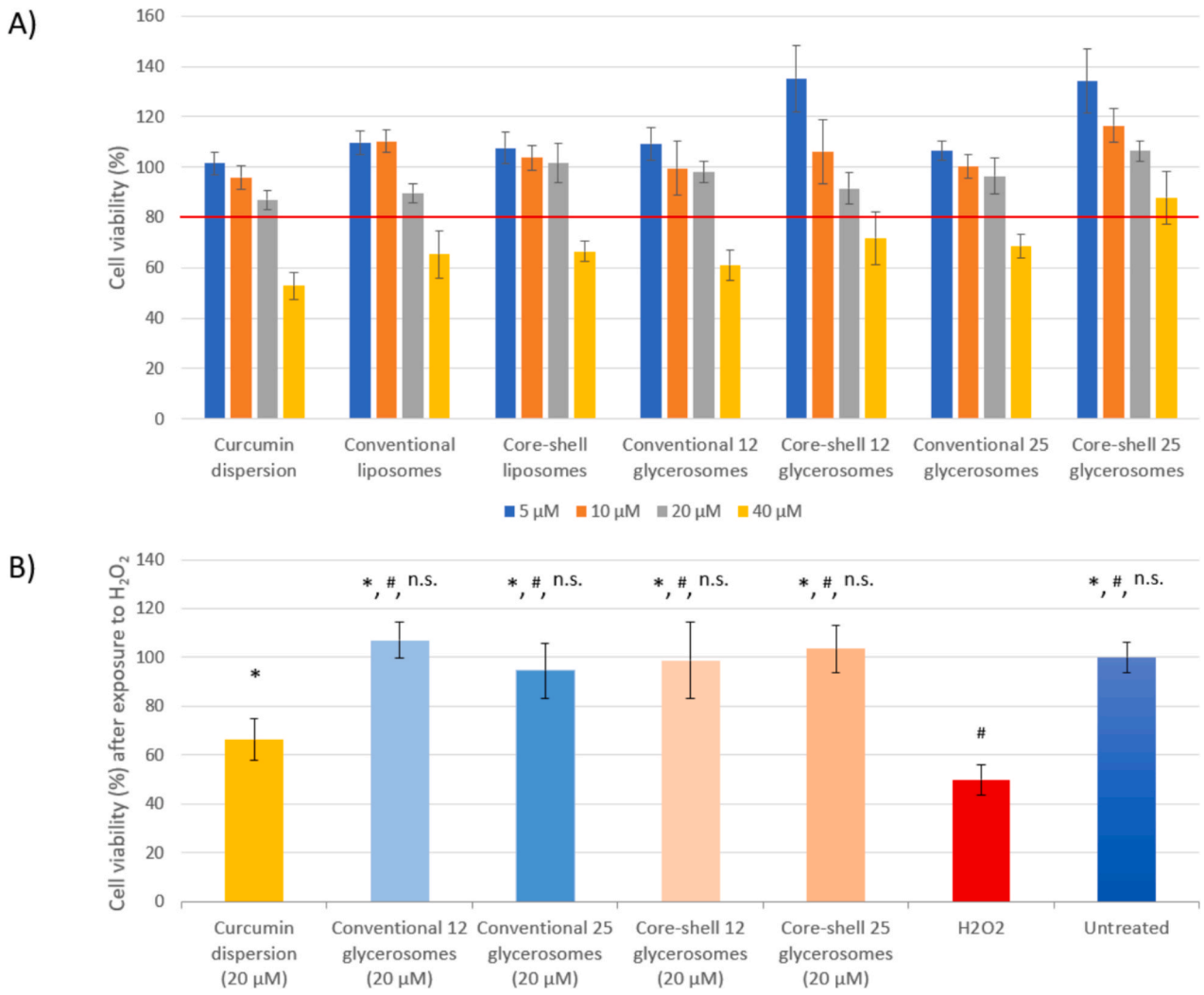

Fig. 3. Viability of A549 cells: A) exposed to curcumin (5–40 μM) in dispersion or loaded in conventional or core–shell nanocarriers; B) stressed with hydrogen peroxide and exposed to curcumin (20 μM) in dispersion or loaded in conventional or core–shell nanocarriers. Untreated cells served as a positive control, whereas cells exposed to H_2O_2 without curcumin treatment served as an oxidative stress control (negative control). Data are presented as mean values ± standard deviations (n = 8). * $p < 0.05$ vs negative control. # $p < 0.05$ vs curcumin dispersion.

findings support the proposed core–shell organization.

From the aerosolization studies, the conventional and core–shell 25 glycerosomes stood out as the most promising formulations, displaying a high degree of aerosolization (DF ~ 96%), high Fine Particle Fraction (> 85%), and MMAD values within the optimal range for targeted lung delivery (~4.1 μm). By contrast, the highest glycerol concentration (50% w/v) reduced the aerosolization performance to values comparable to those obtained by Melis and co-workers using the same glycerol concentration (Melis et al., 2016). Prior research has established that all nebulizers exhibit a viscosity threshold beyond which nebulization efficiency dramatically decreases (Weber et al., 1997; Steckel et al., 2003). A glycerol concentration of 50% w/v likely exceeded this threshold for the Pari Boy nebulizer, resulting in reduced performance and suboptimal DF values for conventional and core–shell 50 glycerosomes (~47 and ~ 55%, respectively). Conversely, the complete omission of glycerol also yielded suboptimal results. Specifically, although conventional and core–shell liposomes displayed MMAD values < 5 μm, DF ≥ 80%, and FPF of ~ 67–72%, they were outperformed by conventional and core–shell 12 and 25 glycerosomes. Thus, the increased viscosity imparted by glycerol at 12.5–25% w/v concentrations appeared to be optimal, yielding MMAD values of 4.0–4.2 μm and supporting efficient lung deposition of curcumin. In clinical settings, formulations enhancing target-site deposition of therapeutic agents can improve outcomes, reduce dosing frequency, and limit systemic toxicity (Hu et al., 2024; Loo et al., 2023). Furthermore, when endowed with an adequate viscosity, they might prolong residence time and support sustained therapeutic effects.

The biocompatibility investigations on both A549 and 16HBE cell lines revealed that curcumin-loaded nanocarriers were well tolerated at curcumin concentrations ≤ 20 μM, which were non-cytotoxic on both cell lines. The present findings are consistent with the results reported by multiple research groups studying curcumin-loaded nanocarriers on the same cell lines and at comparable concentrations (Altube et al., 2021; Rastegar-Pouyani et al., 2025; Zhang et al., 2018).

Once the non-cytotoxic concentrations were established, the formulations having the best biocompatibility and aerosolization profiles – namely conventional and core–shell 25 glycerosomes – were further characterized *in vitro*. Specifically, it was further investigated the ability of curcumin-loaded conventional and core–shell 25 glycerosomes to: 1) counteract reactive oxygen species production in A549 widely used model for human alveolar epithelial cells, especially Type II (ATII) cells (Rastegar-Pouyani et al., 2025), which serve as a suitable model to study mechanisms of drug delivery at the pulmonary epithelium and oxidative stress in the lungs and 2) mitigate the inflammation induced by cigarette smoke extract in 16HBE bronchial cells, which represent a model that reproduces bronchial epithelial cells that are the first barrier against

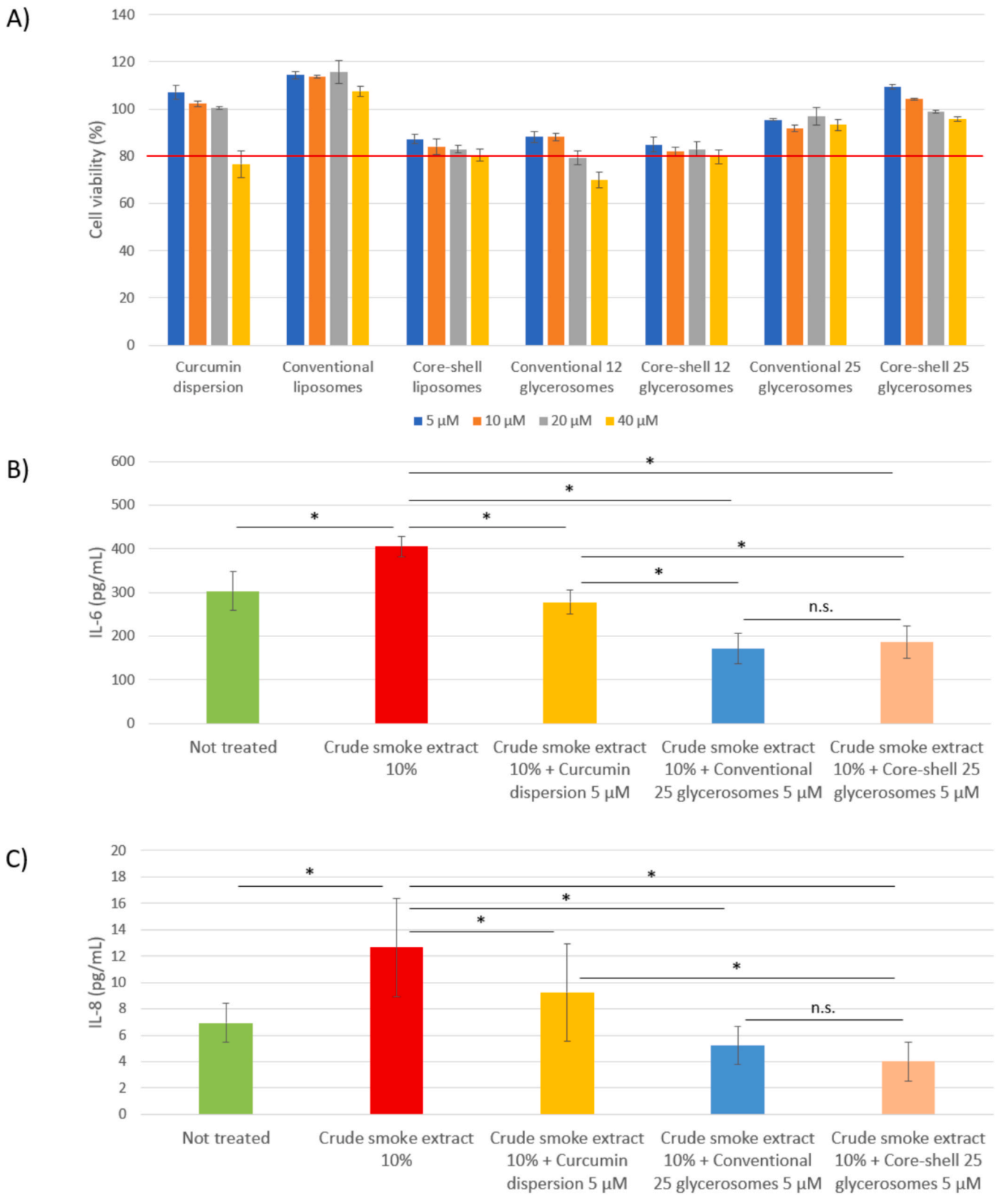

Fig. 4. A) Viability of 16HBE cells exposed to curcumin (5–40 µM) in dispersion or loaded in conventional or core–shell nanocarriers; B and C) Expression of the pro-inflammatory cytokines IL-6 and IL-8 by 16HBE cells exposed to curcumin (5 µM) in dispersion or loaded in conventional or core–shell nanocarriers. Data are presented as mean values ± standard deviations (n = 8). * $p < 0.05$ for the pairwise comparisons indicated by brackets; n.s. $p > 0.05$ for the pairwise comparisons indicated by brackets.

environmental insults and so the first cells to encounter the toxic compounds delivered by smoke.

The A549 cells were exposed to hydrogen peroxide, a well-known oxidative stressor. Under these conditions, conventional and core–shell 25 glycerosomes exhibited a higher capacity to counteract oxidative stress compared to curcumin in dispersion, emphasizing the advantages of the nanocarrier system over the free drug. This finding supports the previous work of Manca et al., who explored the use of different polymer glycerosomes to harness the antioxidant properties of curcumin (Manca et al., 2015).

To study the anti-inflammatory potential, 16HBE cells were exposed to cigarette smoke extract, mimicking the oxidative and inflammatory condition of the lungs upon inhalation of cigarette smoke. Cigarette smoke exposure is known to influence the inflammatory responses of respiratory cells by modulating the production of various potent pro-inflammatory cytokines and chemokines. This leads to the recruitment of macrophages and neutrophils, resulting in further damage to the lung tissue. Among the cytokines, exposure of human bronchial epithelial cell lines to cigarette smoke has been shown to increase the release of the neutrophil chemoattractant IL-8 and the pro-inflammatory cytokine IL-6. In the present study, curcumin-loaded conventional and core–shell 25 glycerosomes significantly attenuated the increased release of both IL-6 and IL-8 compared to control cells exposed to cigarette smoke extract. In addition, they were more effective than the curcumin dispersion, suggesting that glycerosomes can enhance the anti-inflammatory properties of curcumin in fair agreement with previous studies (Paranjpe and Müller-Goymann, 2014; Zanotto-Filho et al., 2013).

5. Conclusions

This study demonstrates that curcumin-loaded conventional and core–shell 25 glycerosomes hold promise as innovative inhalable delivery systems to counteract oxidative stress and inflammation in the lungs. These nanocarriers displayed excellent aerosolization properties and were well-tolerated by both lung epithelial and bronchial cells. Moreover, they exhibited a higher capacity to mitigate oxidative stress and attenuate the release of pro-inflammatory cytokines compared to the free drug. Further studies are needed to fully elucidate the mechanisms underlying the superior biological activity of these innovative systems, evaluate their *in vivo* performance, and establish the long-term effects of chronic inhalation exposure.

CRediT authorship contribution statement

Matteo Aroffu: Writing – review & editing, Writing – original draft, Methodology, Investigation, Formal analysis, Data curation. **Pietro Matricardi:** Writing – review & editing, Writing – original draft, Formal analysis, Data curation. **Chiara Di Meo:** Writing – review & editing, Writing – original draft, Formal analysis, Data curation. **Donatella Valenti:** Writing – original draft, Methodology, Formal analysis, Data curation. **Maria Ferraro:** Methodology, Investigation, Formal analysis, Data curation. **Elisabetta Pace:** Investigation, Formal analysis, Data curation. **Amparo Nacher:** Methodology, Investigation, Formal analysis, Data curation. **Iris Usach:** Writing – original draft, Methodology, Investigation, Formal analysis, Data curation. **José Esteban Peris:** Methodology, Investigation, Formal analysis, Data curation. **Octavio Diez-Sales:** Writing – original draft, Formal analysis, Data curation. **Visar Malaj:** Writing – original draft, Formal analysis, Data curation. **Rita Abi Rached:** Writing – original draft, Investigation, Data curation. **Jose Luis Pedraz:** . **Ines Castangia:** Writing – review & editing, Writing – original draft, Investigation. **Maria Manconi:** Writing – review & editing, Writing – original draft, Supervision, Formal analysis, Data curation, Conceptualization. **Maria Letizia Manca:** Writing – review & editing, Writing – original draft, Validation, Supervision, Methodology, Formal analysis, Data curation, Conceptualization.

Funding

This research received no external funding.

Declaration of competing interest

The authors declare that they have no known competing financial interests or personal relationships that could have appeared to influence the work reported in this paper.

Data availability

No data was used for the research described in the article.

References

Aati, S., Farouk, H.O., Elkarmalawy, M.H., Aati, H.Y., Tolba, N.S., Hassan, H.M., Rateb, M.E., Hamad, D.S., 2024. Intratracheal administration of itraconazole-loaded hyaluronated glycerosomes as a promising nanoplatform for the treatment of lung cancer: formulation, physiochemical, and in vivo distribution. Pharmaceutics 16, 1432. https://doi.org/10.3390/pharmaceutics16111432.

Altube, M.J., Caimi, L.I., Huck-Iriart, C., Morilla, M.J., Romero, E.L., 2021. Reparation of an inflamed air-liquid interface cultured A549 cells with nebulized nanocurcumin. Pharmaceutics 13, 1331. https://doi.org/10.3390/pharmaceutics13091331.

Aoshiba, K., Nagai, A., 2003. Oxidative stress, cell death, and other damage to alveolar epithelial cells induced by cigarette smoke. Tob. Induc. Dis. 1, 219–226. https://doi.org/10.1186/1617-9625-1-3-219.

Arauzo, B., Lopez-Mendez, T.B., Lobera, M.P., Calzada-Funes, J., Pedraz, J.L., Santamaria, J., 2021. Excipient-free inhalable microparticles of azithromycin produced by electrospray: a novel approach to direct pulmonary delivery of antibiotics. Pharmaceutics 13, 1988. https://doi.org/10.3390/pharmaceutics13121988.

Aroffu, M., Manca, M.L., Pedraz, J.L., Manconi, M., 2023. Liposome-based vaccines for minimally or noninvasive administration: an update on current advancements. Expert Opin. Drug Deliv. 20, 1573–1593. https://doi.org/10.1080/17425247.2023.2288856.

Aroffu, M., Abi Rached, R., Castangia, I., Italiani, P., D'Apice, L., Fernàndez-Busquets, X., Nacher, A., Manconi, M., Pedraz, J.L., Manca, M.L., 2024. A preliminary investigation on hydrogel disks imbibed with enriched transfersomes as promising tool to promote the cutaneous deposition of vaccine antigens. J. Drug Delivery Sci. Technol. 102, 106399. https://doi.org/10.1016/j.jddst.2024.106399.

Aroffu, M., Sainz-Ramos, F., García-Villén, F., Fernàndez-Busquets, X., Manconi, M., Pedraz, J.L., Manca, M.L., Fadda, A.M., 2025. Liposomal sprays for nasal vaccination: a comparative study of cationic and anionic formulations involving stability upon nebulization, sprayability, and in vitro immune activation. J. Drug Delivery Sci. Technol. 114, 107498. https://doi.org/10.1016/j.jddst.2025.107498.

Barnes, P.J., 2020. Oxidative stress-based therapeutics in COPD. Redox Biol. 33, 101544. https://doi.org/10.1016/j.redox.2020.101544.

Bors, W., Michel, C., 2002. Chemistry of the antioxidant effect of polyphenols. Ann. N. Y. Acad. Sci. 957, 57–69. https://doi.org/10.1111/j.1749-6632.2002.tb02905.x.

Castangia, I., Manca, M.L., Catalán-Latorre, A., Maccioni, A.M., Fadda, A.M., Manconi, M., 2016. Phycocyanin-encapsulating hyalurosomes as carrier for skin delivery and protection from oxidative stress damage. J. Mater. Sci. - Mater. Med. 27, 1–10. https://doi.org/10.1007/s10856-016-5687-4.

Chen, Q., Wang, Y., Xu, K., Lu, G., Ying, Z., Wu, L., Zhan, J., Fang, R., Wu, Y., Zhou, J., 2010. Curcumin induces apoptosis in human lung adenocarcinoma A549 cells through a reactive oxygen species-dependent mitochondrial signaling pathway. Oncol. Rep. 23, 397–403.

Casula, E., Manca, M.L., Perra, M., Pedraz, J.L., Lopez-Mendez, T.B., Lozano, A., Calvo, E., Zaru, M., Manconi, M., 2021. Nasal spray formulations based on combined hyalurosomes and glycerosomes loading *Zingiber officinale* extract as green and natural strategy for the treatment of rhinitis and rhinosinusitis. Antioxidants 10, 1109. https://doi.org/10.3390/antiox10071109.

Duplessis, J., Ramachandran, C., Weiner, N., Muller, D., 1996. The influence of lipid composition and lamellarity of liposomes on the physical stability of liposomes upon storage. Int. J. Pharm. 127, 273–278. https://doi.org/10.1016/0378-5173(95)04281-4.

Enaru, B., Socaci, S., Farcas, A., Socaciu, C., Danciu, C., Stanila, A., Diaconeasa, Z., 2021. Novel delivery systems of polyphenols and their potential health benefits. Pharmaceuticals 14, 946. https://doi.org/10.3390/ph14100946.

European Pharmacopeia 9.0 2.9.44. Preparations For Nebulisation - Characterisation, n. d.

Fanoudi, S., Alavi, M.S., Mehri, S., Hosseinzadeh, H., 2024. The protective effects of curcumin against cigarette smoke-induced toxicity: a comprehensive review. Phytother. Res. 38, 98–116. https://doi.org/10.1002/ptr.8035.

Ferraro, M., Di Vincenzo, S., Dino, P., Bucchieri, S., Cipollina, C., Gjomarkaj, M., Pace, E., 2019. Budesonide, Aclidinium and Formoterol in combination limit inflammaging processes in bronchial epithelial cells exposed to cigarette smoke. Exp. Gerontol. 118, 78–87. https://doi.org/10.1016/j.exger.2019.01.016.

Foster, K.A., Oster, C.G., Mayer, M.M., Avery, M.L., Audus, K.L., 1998. Characterization of the A549 cell line as a type II pulmonary epithelial cell model for drug metabolism. Exp. Cell Res. 243, 359–366. https://doi.org/10.1006/excr.1998.4172.

Fröhlich, E., Mercuri, A., Wu, S., Salar-Behzadi, S., 2016. Measurements of deposition, lung surface area and lung fluid for simulation of inhaled compounds. Front. Pharmacol. 7. https://doi.org/10.3389/fphar.2016.00181.

Fulgheri, F., Aroffu, M., Ramírez, M., Román-Álamo, L., Peris, J.E., Usach, I., Nacher, A., Manconi, M., Fernàndez-Busquets, X., Manca, M.L., 2023a. Curcumin or quercetin loaded nutriosomes as oral adjuvants for malaria infections. Int. J. Pharm. 643, 123195. https://doi.org/10.1016/j.ijpharm.2023.123195.

Fulgheri, F., Manca, M.L., Fernàndez-Busquets, X., Manconi, M., 2023b. Analysis of complementarities between nanomedicine and phytodrugs for the treatment of malarial infection. Nanomedicine. https://doi.org/10.2217/nnm-2023-0116.

García, F.J.G., Andreo, A.R., Manconi, M., Manca, M.L., Matricardi, P., di Meo, C., Fernàndez-Busquets, X., Díaz, F.M., Salmerón, D., Jornet, P.L., 2025. In vitro and in vivo efficacy evaluation of new self-assembling curcumin loaded nanohyaluronan-glycerosomes on wound restoring in health and diabetic rats. Int. J. Biol. Macromol. 315, 144699. https://doi.org/10.1016/j.ijbiomac.2025.144699.

Gruber, A., Joshi, A.A., Graff, P., Cuéllar-Camacho, J.L., Hedtrich, S., Klinger, D., 2022. Influence of nanogel amphiphilicity on dermal delivery: balancing surface hydrophobicity and network rigidity. Biomacromolecules 23, 112–127. https://doi.org/10.1021/acs.biomac.1c01100.

Hu, Y., Sheng, Y., Liu, P., Sun, J., Tang, L., 2024. The pharmacokinetics and tissue distribution of curcumin following inhalation administration in rats – a comparative analysis with oral and intravenous routes. Biomed. Chromatogr. 38, e6003.

Hussain, Z., Akbari, A.H., Barbuor, S.H., Dawood Alshetiwi, D.S., Ahmed, I.S., Rawas-Qalaji, M., 2024. Hyaluronic acid based functionalization of nanodelivery systems: a promising strategy for CD44-receptors-mediated targeted therapy of lung cancer. J. Drug Deliv. Sci. Technol. 101, 106183. https://doi.org/10.1016/j.jddst.2024.106183.

Janciauskiene, S., 2020. The beneficial effects of antioxidants in health and diseases. Chronic Obstructive Pulmonary Dis.: J. COPD Foundat., 7, 182–202. 10.15326/jcopdf.7.3.2019.0152.

Kalpana, C., Sudheer, A.R., Rajasekharan, K.N., Menon, V.P., 2007. Comparative effects of curcumin and its synthetic analogue on tissue lipid peroxidation and antioxidant status during nicotine-induced toxicity. Singapore Med. J. 48, 124–130.

Kozlowska, J., Pauter, K., Sionkowska, A., 2018. Carrageenan-based hydrogels: effect of sorbitol and glycerin on the stability, swelling and mechanical properties. Polym. Test. 67, 7–11. https://doi.org/10.1016/j.polymertesting.2018.02.016.

Le, Z., Liu, Z., Sun, L., Liu, L., Chen, Y., 2020. Augmenting therapeutic potential of polyphenols by hydrogen-bonding complexation for the treatment of acute lung inflammation. ACS Appl. Bio Mater. 3, 5202–5212. https://doi.org/10.1021/acsabm.0c00616.

Li, Q., Sun, J., Mohammadtursun, N., Wu, J., Dong, J., Li, L., 2019. Curcumin inhibits cigarette smoke-induced inflammation via modulating the PPARγ–NF-κB signaling pathway. Food Funct. 10, 7983–7994. https://doi.org/10.1039/c9fo02159k.

Lin, S.S., Lai, K.C., Hsu, S.C., Yang, J.S., Kuo, C.L., Lin, J.P., Ma, Y.S., Wu, C.C., Chung, J. G., 2009. Curcumin inhibits the migration and invasion of human A549 lung cancer cells through inhibition of matrix metalloproteinase-2 and -9 and vascular endothelial growth factor (VEGF). Cancer Lett. 285, 127–133. https://doi.org/10.1016/j.canlet.2009.04.037.

Lelli, D., Sahebkar, A., Johnston, T.P., Pedone, C., 2017. Curcumin use in pulmonary diseases: State of the art and future perspectives. Pharmacol. Res. 115, 133–148. https://doi.org/10.1016/j.phrs.2016.11.017.

Liu, F., Gao, S., Yang, Y., Zhao, X., Fan, Y., Ma, W., Yang, D., Yang, A., Yu, Y., 2018. Antitumor activity of curcumin by modulation of apoptosis and autophagy in human lung cancer A549 cells through inhibiting PI3K/Akt/mTOR pathway. Oncol. Rep. 39, 1523–1531. https://doi.org/10.3892/or.2018.6188.

Loo, C.Y., Traini, D., Young, P.M., Parumasivam, T., Lee, W.H., 2023. Pulmonary delivery of curcumin and quercetin nanoparticles for lung cancer – Part 1: Aerosol performance characterization. J. Drug Delivery Sci. Technol. 86, 104646. https://doi.org/10.1016/j.jddst.2023.104646.

Lukhele, B.S., Bassey, K., Witika, B.A., 2023. The utilization of plant-material-loaded vesicular drug delivery systems in the management of pulmonary diseases. Curr. Issues Mol. Biol. 45, 9985–10017. https://doi.org/10.3390/cimb45120624.

Manca, M.L., Peris, J.E., Melis, V., Valenti, D., Cardia, M.C., Lattuada, D., Escribano-Ferrer, E., Fadda, A.M., Manconi, M., 2015. Nanoincorporation of curcumin in polymer-glycerosomes and evaluation of their in vitro–in vivo suitability as pulmonary delivery systems. RSC Adv. 5, 105149–105159. https://doi.org/10.1039/C5RA24032H.

Manca, M.L., Zaru, M., Manconi, M., Lai, F., Valenti, D., Sinico, C., Fadda, A.M., 2013. Glycerosomes: a new tool for effective dermal and transdermal drug delivery. Int. J. Pharm. 455, 66–74. https://doi.org/10.1016/j.ijpharm.2013.07.060.

Mandal, B., Bhattacharjee, H., Mittal, N., Sah, H., Balabathula, P., Thoma, L.A., Wood, G. C., 2013. Core–shell-type lipid–polymer hybrid nanoparticles as a drug delivery platform. Nanomedicine 9, 474–491. https://doi.org/10.1016/j.nano.2012.11.010.

Melis, V., Manca, M.L., Bullita, E., Tamburini, E., Castangia, I., Cardia, M.C., Valenti, D., Fadda, A.M., Peris, J.E., Manconi, M., 2016. Inhalable polymer-glycerosomes as safe and effective carriers for rifampicin delivery to the lungs. Colloids Surf. B Biointerfaces 143, 301–308. https://doi.org/10.1016/j.colsurfb.2016.03.044.

Montanari, E., Capece, S., Di Meo, C., Meringolo, M., Coviello, T., Agostinelli, E., Matricardi, P., 2013. Hyaluronic acid nanohydrogels as a useful tool for BSAO immobilization in the treatment of melanoma cancer cells. Macromol. Biosci. 13, 1185–1194. https://doi.org/10.1002/mabi.201300114.

Montanari, E., Di Meo, C., Sennato, S., Francioso, A., Marinelli, A.L., Ranzo, F., Schippa, S., Coviello, T., Bordi, F., Matricardi, P., 2017. Hyaluronan-cholesterol nanohydrogels: Characterisation and effectiveness in carrying alginate lyase. N. Biotechnol. 37, 80–89. https://doi.org/10.1016/j.nbt.2016.08.004.

Muller, A.G., Sarker, S.D., Saleem, I.Y., Hutcheon, G.A., 2019. Delivery of natural phenolic compounds for the potential treatment of lung cancer. DARU J. Pharmaceutical Sci. 27, 433–449. https://doi.org/10.1007/s40199-019-00267-2.

Nikjoo, D., van der Zwaan, I., Brülls, M., Tehler, U., Frenning, G., 2021. Hyaluronic acid hydrogels for controlled pulmonary drug delivery—a particle engineering approach. Pharmaceutics 13, 1878. https://doi.org/10.3390/pharmaceutics13111878.

Oelschlaeger, C., Bossler, F., Willenbacher, N., 2016. Synthesis, structural and micromechanical properties of 3D hyaluronic acid-based cryogel scaffolds. Biomacromolecules 17, 580–589. https://doi.org/10.1021/acs.biomac.5b01529.

Paranjpe, M., Müller-Goymann, C., 2014. Nanoparticle-mediated pulmonary drug delivery: a review. Int. J. Mol. Sci. 15, 5852–5873. https://doi.org/10.3390/ijms15045852.

Patton, J.S., 2004. The lungs as a portal of entry for systemic drug delivery. Proc. Am. Thorac. Soc. 1, 338–344. https://doi.org/10.1513/pats.200409-049TA.

Rached, R.A., Shakya, A.K., Fulgheri, F., Aroffu, M., Castangia, I., García-Villén, F., Ferraro, M., Fernàndez-Busquets, X., Pedraz, J.L., Louka, N., Maroun, R.G., Manconi, M., Manca, M.L., 2025. Resveratrol and grape pomace extract incorporated in modified phospholipid vesicles: a potential strategy to mitigate cigarette smoke-induced oxidative stress. Free Radic. Biol. Med. 230, 151–162. https://doi.org/10.1016/j.freeradbiomed.2025.02.009.

Rastegar-Pouyani, N., Dongsar, T.S., Ataei, M., Hassani, S., Gumpricht, E., Kesharwani, P., Sahebkar, A., 2025. An overview of the efficacy of inhaled curcumin: a new mode of administration for an old molecule. Expert Opin. Drug Deliv. 1–16. https://doi.org/10.1080/17425247.2024.2358880.

Rogers, L.K., Cismowski, M.J., 2018. Oxidative stress in the lung – the essential paradox. Curr. Opin Toxicol. 7, 37–43. https://doi.org/10.1016/j.cotox.2017.09.001.

Ruwizhi, N., Aderibigbe, B.A., 2020. The efficacy of cholesterol-based carriers in drug delivery. Molecules 25, 4330. https://doi.org/10.3390/molecules25184330.

Shailendiran, D., Pawar, N., Chanchal, A., Pandey, R.P., Bohidar, H.B., Verma, A.K., 2011. Characterization and Antimicrobial activity of Nanocurcumin and Curcumin. In: In: 2011 International Conference on Nanoscience, Technology and Societal Implications. IEEE, pp. 1–7. https://doi.org/10.1109/NSTSI.2011.6111984.

Steckel, H., Eskandar, F., Witthohn, K., 2003. Effect of excipients on the stability and aerosol performance of nebulized aviscumine. J. Aerosol Med. 16, 417–432. https://doi.org/10.1089/089426803772455677.

Teng, H., Chen, L., 2019. Polyphenols and bioavailability: an update. Crit. Rev. Food Sci. Nutr. 59, 2040–2051. https://doi.org/10.1080/10408398.2018.1437023.

Valavanidis, A., Vlachogianni, T., Fiotakis, K., 2009. Tobacco smoke: involvement of reactive oxygen species and stable free radicals in mechanisms of oxidative damage, carcinogenesis and synergistic effects with other respirable particles. Int. J. Environ. Res. Public Health 6, 445–462. https://doi.org/10.3390/ijerph6020445.

Weber, A., Morlin, G., Cohen, M., Williams-Warren, J., Ramsey, B., Smith, A., 1997. Effect of nebulizer type and antibiotic concentration on device performance. Pediatr. Pulmonol. 23, 249–260. https://doi.org/10.1002/(SICI)1099.

Yong, J., Shu, H., Zhang, X., Yang, K., Luo, G., Yu, L., Li, J., Huang, H., 2024. Natural products-based inhaled formulations for treating pulmonary diseases. Int. J. Nanomed. 19, 1723–1748. https://doi.org/10.2147/IJN.S451206.

Zanotto-Filho, A., Coradini, K., Braganhol, E., Schröder, R., de Oliveira, C.M., Simões-Pires, A., Battastini, A.M.O., Pohlmann, A.R., Guterres, S.S., Forcelini, C.M., Beck, R. C.R., Moreira, J.C.F., 2013. Curcumin-loaded lipid-core nanocapsules as a strategy to improve pharmacological efficacy of curcumin in glioma treatment. Eur. J. Pharm. Biopharm. 83, 156–167. https://doi.org/10.1016/j.ejpb.2012.10.019.

Zhang, T., Chen, Y., Ge, Y., Hu, Y., Li, M., Jin, Y., 2018. Inhalation treatment of primary lung cancer using liposomal curcumin dry powder inhalers. Acta Pharm. Sin. B 8, 440–448. https://doi.org/10.1016/j.apsb.2018.03.004.

Zhao, Y., He, Z., Gao, H., Tang, H., He, J., Guo, Q., Zhang, W., Liu, J., 2018. Fine tuning of core–shell structure of hyaluronic acid/cell-penetrating peptides/siRNA nanoparticles for enhanced gene delivery to macrophages in antiatherosclerotic therapy. Biomacromolecules 19, 2944–2956. https://doi.org/10.1021/acs.biomac.8b00501.

Zuo, L., Wijegunawardana, D., 2021. Redox Role of ROS and Inflammation in Pulmonary Diseases. pp. 187–204. 10.1007/978-3-030-68748-9_11.